

# White matter network alterations in patients with depersonalization/derealization disorder

Anika Sierk, PhD (candidate)\*; Judith K. Daniels, PhD\*; Antje Manthey; Jelmer G. Kok, PhD; Alexander Leemans, PhD; Michael Gaebler, PhD; Jan-Peter Lamke, PhD; Johann Kruschwitz, PhD; Henrik Walter, PhD

Published online first on June 6, 2018; subject to revision

**Background:** Depersonalization/derealization disorder (DPD) is a chronic and distressing condition characterized by detachment from oneself and/or the external world. Neuroimaging studies have associated DPD with structural and functional alterations in a variety of distinct brain regions. Such local neuronal changes might be mediated by altered interregional white matter connections. However, to our knowledge, no research on network characteristics in this patient population exists to date. **Methods:** We explored the structural connectome in 23 individuals with DPD and 23 matched, healthy controls by applying graph theory to diffusion tensor imaging data. Mean interregional fractional anisotropy (FA) was used to define the network weights. Group differences were assessed using network-based statistics and a link-based controlling procedure. **Results:** Our main finding refers to lower FA values within left temporal and right temporoparietal regions in individuals with DPD than in healthy controls when using a link-based controlling procedure. These links were also associated with dissociative symptom severity and could not be explained by anxiety or depression scores. Using network-based statistics, no significant results emerged. However, we found a trend for 1 subnetwork that may support the model of frontolimbic dysbalance suggested to underlie DPD symptomatology. **Limitations:** To ensure ecological validity, patients with certain comorbidities or psychotropic medication were included in the study. Confirmatory replications are necessary to corroborate the results of this explorative investigation. **Conclusion:** In patients with DPD, the structural connectivity between brain regions crucial for multimodal integration and emotion regulation may be altered. Aberrations in fibre tract communication seem to be not solely a secondary effect of local grey matter volume loss, but may present a primary pathophysiology in patients with DPD.

## Introduction

Depersonalization/derealization disorder (DPD) is a dissociative disorder<sup>1</sup> estimated to affect 1%–2% of the general population.<sup>2</sup> However, a German study found a 12-month prevalence of 0.007 based on diagnoses given by clinicians, which suggests DPD is severely underdiagnosed, making research challenging in this population.<sup>3</sup> Individuals with DPD experience recurrent episodes of feeling detached from oneself (depersonalization) and/or the external world (derealization). Other clinical phenomena of DPD include emotional numbing and somatosensory distortions.<sup>4,5</sup> Shorter episodes of depersonalization or derealization can also occur in the context of other disorders, such as temporal lobe epilepsy,<sup>6</sup> schizophrenia,<sup>7</sup> or posttraumatic stress disorder (PTSD).<sup>8</sup> Psychophysiological

and neuroimaging research suggests DPD to be underpinned by alterations within neurobiological circuits: an early model emphasizing the role of the temporal lobes<sup>9</sup> has been supported by studies with epileptic patients<sup>10,11</sup> and 2 neuroimaging studies on DPD.<sup>12,13</sup> A more recent theory proposes a frontolimbic dysbalance in individuals with DPD, assuming hyperactive prefrontal cortices to inhibit limbic structures,<sup>14</sup> which is also congruent with theories proposed for the dissociative subtype of PTSD.<sup>8,15</sup> Most functional MRI (fMRI) studies on DPD used affective stimuli to test this model and reported hypoactivity in limbic regions<sup>16,17</sup> and hyperactivation in prefrontal regions in individuals with DPD compared with healthy controls,<sup>17,18</sup> (but also see Medford and colleagues<sup>19</sup>). Unfortunately, all fMRI studies published to date had very small DPD sample sizes ( $n = 6–14$ ), which severely affects their

**Correspondence to:** J. Daniels, Department of Clinical Psychology and Experimental Psychopathology, University of Groningen, Grote Kruisstraat 2, 9712 TS Groningen, Netherlands; J.K.Daniels@rug.nl

Submitted June 7, 2017; Revised Dec. 1, 2017; Accepted Jan. 21, 2018

\*These authors contributed equally to this work.

DOI: 10.1503/jpn.170110

© 2018 Joule Inc. or its licensors

validity. Two recent structural MRI studies with larger samples of patients with DPD and healthy controls suggest that grey matter alterations underlie DPD symptomatology.<sup>12,20</sup> One of them ( $n = 20$  patients with DPD) found less cortical thickness in the right middle temporal gyrus,<sup>12</sup> while the other ( $n = 25$  patients with DPD) found reductions of grey matter volume in the right caudate, right thalamus and right cuneus as well as volume increases in the left dorsomedial prefrontal cortex and right somatosensory regions.<sup>20</sup> In the context of other disorders, dissociation has also been associated with altered functional connectivity.<sup>21</sup> Edelman and Tononi<sup>22</sup> suggest that disturbed neuronal interaction might underlie the cognitive and emotional disconnect characteristic of dissociation. As dissociative symptoms constitute the hallmark of DPD, one may hypothesize that disturbed integration of neuronal information underlies DPD symptomatology as well. However, to our knowledge, no study to date has analyzed functional connectivity (except in a single case study<sup>23</sup>) or structural connectivity (i.e., white matter anatomy) in patients with DPD.

Diffusion tensor imaging (DTI) allows the human brain connectome to be imaged noninvasively.<sup>24,25</sup> Applying graph theory to DTI data has made it possible to analyze structural connectivity on a network level.<sup>26</sup> Graph theory is a mathematical approach for the analysis of complex networks constructed of “nodes” (i.e., in our case brain regions of interest), which are interconnected via “edges.” Graph theory has emerged as a powerful tool for identifying anatomically localized subnetworks associated with neuronal alterations in psychiatric conditions.<sup>27–30</sup> By applying an exploratory graph theoretical analysis on diffusion MRI tractography data, we sought to identify networks with different structural connectivity between patients with DPD and matched healthy controls. Thus, the research question of the present study is whether DPD is associated with altered structural connectivity on a network level.

Despite existing theories on the underlying neurobiology of DPD, empirical evidence is scarce. Being the first group, to our knowledge, to investigate structural connectivity in patients with DPD, we sought to provide an unbiased investigation. To this end, we chose to use a strictly exploratory approach aimed at theory-building rather than hypothesis-testing as discussed with regard to the replication crisis.<sup>31</sup>

## Methods

### Participants

We acquired DTI scans in patients with DPD and healthy controls, who were a subset of the sample analyzed for volumetric changes in grey matter in an earlier study by our group.<sup>20</sup> Participants were recruited via advertisements posted online and in public spaces as well as in mental health in- and outpatient clinics. We obtained written informed consent from all individuals before participation. All participants were interviewed using German versions of 3 standardized clinical interviews: the Structured Clinical Interview for Dissociative Disorders (SKID-D),<sup>32</sup> the Structured Clinical Interview for DSM-IV (SKID)<sup>33</sup> and the International Personality Disorder Examina-

tion (IPDE).<sup>34</sup> The SKID-D was used to establish the diagnosis of DPD according to the criteria in DSM-IV (300.6) as well as the criteria of the depersonalization-derealization disorder according to ICD-10 (F48.1). The DPD diagnosis established in the present work is still valid, as the relevant criteria have not changed in DSM-5. Patients were excluded from the study if they had a history of lifetime psychotic disorders, substance addiction in remission for less than 6 months, or current PTSD. Patients with comorbid PTSD were excluded to avoid diagnostic ambiguity, considering that symptoms of the dissociative subtype of PTSD strongly overlap with DPD symptoms.<sup>1</sup>

Participants were included in the control group only when no mental disorder had been identified. General exclusion criteria were lifetime neurologic disorders, serious head injury, current use of benzodiazepines or opioids, insufficient knowledge of the German language, and MRI incompatibilities. The study was approved by the research ethics board at the Charité – Universitätsmedizin Berlin.

### Questionnaires and tasks

All participants completed several self-report questionnaires. To assess symptom severity of depersonalization and derealization, participants completed the German versions of the 30-item Cambridge Depersonalization Scale (CDS-30)<sup>35</sup> and the Dissociative Experiences Scale (DES).<sup>36</sup> Patients with a score of at least 60 on the CDS-30 ( $\alpha = 0.981$ ) were invited for clinical diagnostics. In addition, the Beck Depression Inventory (BDI-II),<sup>37</sup> the State-Trait Anxiety Inventory (STAI),<sup>38</sup> the Liebowitz Social Anxiety Scale (LSAS),<sup>39</sup> the Toronto Alexithymia Scale (TAS-20),<sup>40</sup> the Emotion Regulation Questionnaire (ERQ),<sup>41</sup> the Kentucky Inventory of Mindfulness Skills,<sup>42</sup> the questionnaire for functional and dysfunctional self-focused attention,<sup>43</sup> the Sheehan Disability Scale,<sup>44</sup> and the short version of the Childhood Trauma Questionnaire<sup>45</sup> were used for sample characterization. Information processing speed and executive functions were measured using the Trail Making Test versions A and B (TMT),<sup>46</sup> respectively.

### MRI acquisition

We acquired the MRI data using a 3 T Siemens Tim Trio scanner equipped with a 12-channel head coil. Diffusion tensor imaging was performed with a single-shot echo-planar imaging sequence using the following parameters: repetition time (TR) 7500 ms, echo time (TE) 86 ms, 61 slices, voxel size  $2.3 \times 2.3 \times 2.3$  mm<sup>3</sup>, slice thickness 2.3 mm, field of view (FOV)  $220 \times 220$  mm<sup>2</sup>, 64 diffusion directions, b value = 1000s/mm<sup>2</sup>. We acquired  $T_1$ -weighted images using a magnetization-prepared rapid acquisition with gradient echo sequence (TR 1.9 ms, TE 2.52 ms, inversion time (TI) 900 ms, flip angle 9°, FOV  $256 \times 256$  mm<sup>2</sup>, 192 slices, 1 mm isotropic voxel sizes, 50% distancing factor).

### Preprocessing

The preprocessing pipeline for the structural network analysis is shown in Figure 1. We processed the  $T_1$ -weighted MRI scans using the default settings implemented in FreeSurfer

version 5.3 (<https://surfer.nmr.mgh.harvard.edu/>). Important processing steps include skull stripping, segmentation of subcortical white matter and deep grey matter volumetric structures, intensity normalization, definition of the grey matter–white matter boundary, and parcellation of the cerebral cortex into units with respect to gyral and sulcal structures.<sup>47</sup> Each output was visually inspected for quality control. Five scans had to be manually corrected and (partially) rerun. The final results yielded a proper distinction of each surface and subcortical ROIs in all participants.

The preprocessing of the DTI data was performed with ExploreDTI, version 4.8.6 ([www.exploredti.com](http://www.exploredti.com))<sup>48</sup> in MATLAB (Release 2014b; <https://mathworks.com>) using default settings. Specifically, data were corrected for participant motion using “Rekindle” methods,<sup>49</sup> eddy current–induced geometric distortions<sup>50</sup> and EPI distortions.<sup>51</sup> Subsequently, constrained spherical deconvolution (CSD) whole brain tractography was performed<sup>52,53</sup> for each participant. Following visual inspection, 1 participant was excluded as the fibre tracts could not be reconstructed adequately.

### Connectivity matrices

Connectivity matrices were constructed based on 85 pre-defined anatomic regions of interest (ROIs) derived from FreeSurfer. The ROIs encompassed all cortical regions from the Desikan Killiany atlas (34 areas) plus the bilateral subcortical structures hippocampus, amygdala, thalamus, caudate, pallidum, putamen, accumbens area, ventral diencephalon and brainstem. The cerebellum was excluded as it was not fully captured in a number of scans. The 85 ROI files were combined with the streamline files from ExploreDTI, resulting in 85 × 85 connectivity matrices for each participant. It is inevitable when using deterministic tractography that not all fibre tracts can be reconstructed in all

participants.<sup>54,55</sup> As this may vary between groups, we included only links in the network analyses for which streamlines had been generated successfully for all participants (i.e., 1153 links).

### Statistical analysis

We included age, sex, and handedness as covariates in all network analyses; although they did not differ significantly between groups, subtle changes in these variables have been shown to impact structural brain connectivity.<sup>56</sup> We used the streamlines between each pair of nodes as a mask, within which we calculated mean fractional anisotropy (FA), a commonly used parameter that reflects tissue organization in cerebral white matter.<sup>57</sup> Mean FA values were used as edge weights between any 2 ROIs and thus presented an indicator for their strength of association or structural connectivity, respectively. Note that not all included ROI pairs are linked via direct anatomic connections (only homotopic regions are directly connected via fibre bundles) as tractography accounts for indirect connections. All second-level network analyses (i.e., network-based statistics, link-based false discovery rate [FDR] analysis, and correlational analyses with symptom scores) were performed using GraphVar version 1.0 ([www.nitrc.org/projects/graphvar/](http://www.nitrc.org/projects/graphvar/)).<sup>58</sup>

### Network-based statistics: group comparison

Network-based statistics (NBS) is a nonparametric statistical method developed by Zalesky and colleagues<sup>30</sup> to identify graph components within a network that are associated with an external variable, while controlling the family wise error (FWE) rate. Within NBS, statistical thresholding is carried out in 2 steps: first, the hypothesis of interest is tested independently at every connection within a network using link thresholds. Adjacent suprathreshold links may ultimately form

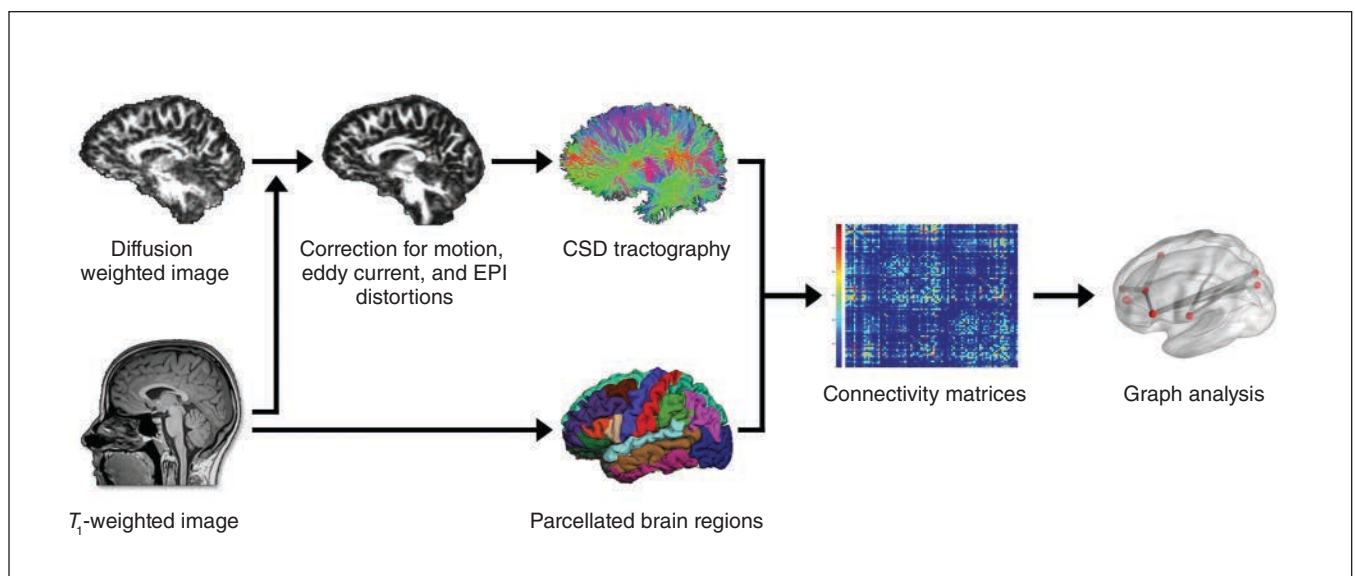


**Fig. 1:** Flowchart of the preprocessing pipeline using FreeSurfer (<https://surfer.nmr.mgh.harvard.edu>) and ExploreDTI ([www.exploredti.com](http://www.exploredti.com)). CSD = constrained spherical deconvolution; EPI = echo-planar imaging.

graph components. Subsequently, the significance of these graph components at the network level is determined by comparing their size against the occurrence of differently sized graph components derived from random data (i.e., by performing FWE correction). In accordance with this procedure, we performed a series of  $t$  tests to identify links between any of the 85 ROIs for which the DPD and control group showed significant differences in FA values. To determine suprathreshold links, we applied descending initial link thresholds ( $l_t$ ) from  $p_{it} = 0.05$  to  $p_{it} = 0.001$  in steps of 0.005. This procedure (i.e., no fixed initial link threshold) was chosen because variations in thresholding can be informative regarding the nature of any observed group difference: effects found only at liberal thresholds (e.g.,  $p_{it} < 0.05$ ) are expected to be subtle and topologically extended, whereas effects evident at conservative thresholds (e.g.,  $p_{it} < 0.001$ ) are likely to reveal strong focal differences between groups.<sup>30</sup> Significance of the resulting graph components was determined by generating a corresponding null-model distribution, using 10 000 permutations. For the present analysis, we considered an identified graph component (i.e., subnetwork) as statistically significant with an FWE-corrected  $p < 0.05$ . However, owing to the explorative nature of this study, significant results are used purely for theory-building and should be replicated with preregistration.<sup>31</sup>

#### Network-based statistics: correlational analysis

To obtain indications of whether the previously described NBS group differences are specific to DPD symptomatology, we subjected the connectivity matrices of all participants (control and DPD) to an NBS partial correlation analysis with dissociative symptom severity, as measured by the CDS-30 (controlling for age, sex and handedness). Specifically, instead of using group-wise  $t$  tests, we applied partial correlations for mass univariate testing in every cell of the connectivity matrix to determine sets of suprathreshold links. Again, significance of the resulting graph components was determined by generating a corresponding null-model distribution with 10 000 random permutations of CDS-30 scores.

#### Link-based analysis using FDR: group comparison

As an additional analysis, we used FDR<sup>59</sup> to explore individual connections between any ROI pair within a network that may be altered in individuals with DPD. Although NBS improves power, as it is a more stringent control of false positives, only the network as a whole can be regarded as significant and, thus, can be interpreted only as a whole. The objective of performing a link-based controlling procedure<sup>30</sup> in addition to using NBS derives from the exploratory nature of the present study; FDR correction may provide additional information on focal effects concerning individual connections. Using FDR, a test statistic and a respective  $p$  value is computed for each network link, which in this case refers to the FA-based connection for which streamlines have successfully been generated in all participants. Therefore, the null hypothesis is tested based on individual links while controlling the ratio of false-positive connections among all positive connections. In contrast, NBS allows rejecting the null hy-

pothesis at the level of cerebral networks by controlling the FWE rate (i.e., the probability of false-positive networks). In the GraphVar toolbox,<sup>58</sup> an FDR correction algorithm<sup>60</sup> is carried out with respect to a designated  $\alpha$  level. We applied an FDR-corrected threshold of  $p_{FDR} = 0.05$  and tested against random groups using 100 000 permutations.

#### Link-based analysis using FDR: correlational analysis

Link-based analysis was performed to explore the association of symptom severity as measured by the CDS-30 with the individual connections between any ROI pair within a network. Again, we computed partial correlations controlling for age, sex and handedness. We applied an FDR-corrected threshold of  $p = 0.05$  and tested against a random distribution of CDS-30 scores using 100 000 permutations.

## Results

### Final sample

We enrolled 24 patients with DPD (18 women) and 23 healthy controls (18 women; Table 1) in the present study; 1 patient had to be excluded owing to inadequate fibre reconstruction, leaving a final sample of 23 patients in the DPD group. Seventeen patients had current comorbid disorders, mainly anxiety disorders, and 9 used psychotropic medication (Table 2).

### Demographics

Patients with DPD did not differ from controls in age ( $t_{44} = 0.289$ ,  $p = 0.77$ ), handedness ( $t_{44} = 1.542$ ,  $p = 0.13$ ), level of education (Mann–Whitney  $U = 245.5$ ,  $p = 0.66$ ), information processing speed, or executive functions (Table 1). Patients with DPD differed significantly from controls on various self-report questionnaires (Table 1), which in turn correlated highly with DPD symptom severity (Appendix 1, Table S1, available at [jpn.ca/170110-a1](http://jpn.ca/170110-a1)). No significant differences between patients with and without psychotropic medication were detected. Information regarding age at symptom onset was available for 21 of 23 patients with DPD. Based on retrospective reports, the mean age at symptom onset was  $18.2 \pm 6.17$  years. At the time of the scan, patients had been living with DPD on average for  $12.43 \pm 10.20$  (range 0.5–36) years. In most cases, symptoms had been chronic since their onset, with either no or only brief interruptions.

### Network-based statistics

#### Group comparison

No significant group differences in graph components (i.e., subnetworks) between brain regions were detected with any of the initial link thresholds. However, a trend was found at an initial link threshold of  $p_{it} = 0.005$ , which indicated group differences regarding 1 subnetwork ( $p_{FWE} = 0.08$  at the network level, controlled for age, sex and handedness). This network comprised 5 nodes and 4 links between frontal and subcortical regions. Within this network, patients with DPD

showed higher FA values than controls between the left superior frontal gyrus, right medial orbitofrontal cortex and its connection to the right amygdala and lower FA values than controls between the right amygdala, brainstem and left caudate (Fig. 2).

### Partial correlation analyses

For 1 patient, no questionnaire data were available, leaving 45 participants for the partial correlation analysis (controlling for age, sex and handedness). No significant correlation between CDS-30 scores and interregional FA values in the links identified using the initial link threshold of  $p_{it} = 0.005$  was found using NBS.

### Link-based analysis using FDR

#### Group comparison

We found that 9 individual graph components significantly differed between patients with DPD and controls when using the link-based controlling procedure (Table 3). Components for which patients with DPD showed lower FA values than controls concerned connections between the left temporal pole and left superior temporal gyrus ( $p_{FDR} < 0.001$ ), between the right middle temporal gyrus and right supramarginal gyrus ( $p_{FDR} = 0.002$ ), between the brainstem and left caudate ( $p_{FDR} < 0.001$ ), between the right medial orbitofrontal cortex and the right caudal anterior cingulate cortex ( $p_{FDR} < 0.001$ ) and between the right inferior temporal gyrus and the right lingual cortex ( $p_{FDR} < 0.001$ ). Higher FA values for patients

with DPD than controls were found for the connection linking the right superior temporal gyrus and the right banks of superior temporal sulcus ( $p_{FDR} < 0.01$ ). Each of the remaining

**Table 2: Current and lifetime comorbid disorders in patients with DPD ( $n = 23$ )**

| Disorder                               | Current, $n$ | Lifetime, $n$ |
|--|--------------|---------------|
| Anxiety disorders                      | 11           | 11            |
| Social anxiety disorder                |              |               |
| Panic disorder                         | 2            | 3             |
| Specific phobia                        | 2            | 2             |
| Obsessive-compulsive disorder          | 2            | 2             |
| Generalized anxiety disorder           | 1            | 1             |
| Mood disorders                         | 2            | 10            |
| Major depressive disorder              |              |               |
| Personality disorders                  | 1            | 1             |
| Emotionally unstable – impulsive type  |              |               |
| Emotionally unstable – borderline type | 1            | 1             |
| Anxious avoidant                       | 1            | 1             |
| Dependent                              | 1            | 1             |
| Other                                  | 0            | 1             |
| Posttraumatic stress disorder          |              |               |
| Conversion disorder                    | 0            | 1             |
| Impulse control disorder               | 1            | 1             |
| Eating disorder                        | 0            | 3             |
| Substance abuse disorder               | 0            | 1             |
| Total comorbidity                      | 17           | 19            |

DPD = depersonalization/derealization disorder.

**Table 1: Demographic characteristics and clinical measures**

| Characteristic | DPD |                     | Control |                     | 2-tailed $t$ test | $p$ value |
|----------------|-----|---------------------|---------|---------------------|-------------------|-----------|
|                | $n$ | Mean $\pm$ SD       | $n$     | Mean $\pm$ SD       |                   |           |
| Age, yr        | 23  | 30.61 $\pm$ 7.31    | 23      | 29.96 $\pm$ 7.99    | $t_{44} = 0.289$  | 0.774     |
| Handedness     | 23  | 0.76 $\pm$ 0.50     | 23      | 0.92 $\pm$ 0.15     | $t_{44} = -1.542$ | 0.135     |
| CDS-30         | 22  | 148.14 $\pm$ 43.10  | 23      | 9.61 $\pm$ 12.04    | $t_{43} = 14.543$ | < 0.001   |
| CDS-State      | 23  | 926.96 $\pm$ 383.52 | 22      | 173.64 $\pm$ 254.40 | $t_{43} = 7.796$  | < 0.001   |
| DES            | 22  | 442.27 $\pm$ 217.95 | 23      | 36.09 $\pm$ 39.05   | $t_{43} = 8.610$  | < 0.001   |
| BDI-II         | 22  | 20.32 $\pm$ 11.27   | 23      | 2.48 $\pm$ 3.41     | $t_{43} = 7.120$  | < 0.001   |
| STAI-T         | 22  | 56.23 $\pm$ 11.80   | 23      | 34.00 $\pm$ 11.37   | $t_{43} = 6.434$  | < 0.001   |
| LSAS           | 22  | 442.27 $\pm$ 217.95 | 23      | 36.09 $\pm$ 39.05   | $t_{43} = 3.738$  | 0.001     |
| TAS-20         | 22  | 55.59 $\pm$ 8.66    | 23      | 52.00 $\pm$ 7.07    | $t_{43} = 5.785$  | < 0.001   |
| ERQ            | 22  | 42.68 $\pm$ 8.98    | 23      | 39.52 $\pm$ 9.62    | $t_{43} = 1.138$  | 0.262     |
| KIMS           | 22  | 86.68 $\pm$ 19.71   | 23      | 124.39 $\pm$ 13.43  | $t_{43} = -7.531$ | < 0.001   |
| DFS            | 22  | 70.36 $\pm$ 9.52    | 23      | 61.65 $\pm$ 9.24    | $t_{43} = 3.119$  | 0.003     |
| CTQ_sum        | 22  | 52.32 $\pm$ 17.52   | 23      | 44.22 $\pm$ 10.33   | $t_{43} = 1.878$  | 0.069     |
| CTQ_PA         | 22  | 6.36 $\pm$ 2.68     | 23      | 5.91 $\pm$ 1.91     | $t_{43} = 0.652$  | 0.518     |
| CTQ_PN         | 22  | 5.50 $\pm$ 2.76     | 23      | 4.00 $\pm$ 1.54     | $t_{43} = 2.241$  | 0.032     |
| CTQ_EA         | 22  | 11.00 $\pm$ 4.04    | 23      | 5.91 $\pm$ 1.91     | $t_{43} = 1.765$  | 0.086     |
| CTQ_EN         | 22  | 6.91 $\pm$ 5.86     | 23      | 4.57 $\pm$ 5.27     | $t_{43} = 1.411$  | 0.165     |
| CTQ_SA         | 22  | 6.45 $\pm$ 2.30     | 23      | 5.65 $\pm$ 1.72     | $t_{43} = 1.119$  | 0.269     |
| TMT-A          | 21  | 24.62 $\pm$ 5.52    | 21      | 24.90 $\pm$ 6.80    | $t_{40} = -0.150$ | 0.882     |
| TMT-B          | 21  | 51.38 $\pm$ 14.20   | 21      | 53.19 $\pm$ 18.59   | $t_{40} = -0.355$ | 0.725     |

BDI = Beck Depression Inventory; CDS = Cambridge Depersonalization Scale; CTQ = Childhood Trauma Questionnaire; DES = Dissociative Experiences Scale; DFS = Questionnaire for functional and dysfunctional self-focused attention; DPD = depersonalization/derealization disorder; EA = emotional abuse; EN = emotional neglect; ERQ = Emotion Regulation Questionnaire; KIMS = Kentucky Inventory of Mindfulness Skills; LSAS = Liebowitz Social Anxiety Scale; PA = physical abuse; PN = physical neglect; SA = sexual abuse; SD = standard deviation; STAI-T = State-Trait Anxiety Scale, trait version; TAS = Toronto Alexithymia Scale, TMT = Trail Making Test.

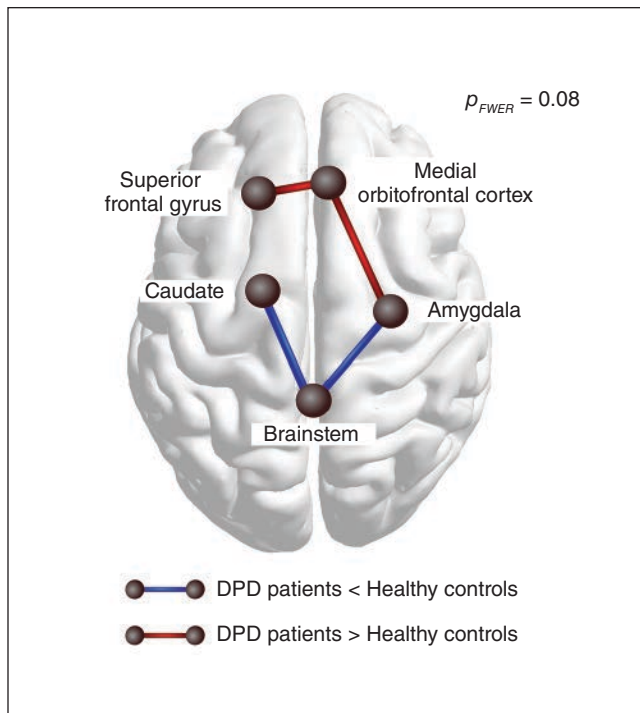


**Fig. 2:** Visualization of the trend found in the group comparison when using network-based statistics. At an initial-link threshold of  $p_{li} = 0.005$ , a subnetwork was identified for which patients with depersonalization/derealization disorder (DPD) displayed lower fractional anisotropy (FA) (blue edges) as well as higher FA (red edges) than healthy controls ( $p_{FWE} = 0.08$ ). Patients showed relatively lower FA values between the left caudate, brainstem and the right amygdala, and higher FA between the left superior frontal gyrus, right medial frontal cortex and the right amygdala. FWE = family-wise error.

3 components encompassed 3 brain regions connected via 2 edges. Patients with DPD showed lower FA values between the left insula, left pars triangularis and the left lateral orbitofrontal cortex ( $p_{FDR} < 0.01$ ), while showing higher FA values between the left isthmus of the cingulate cortex, right cuneus and left superior parietal cortex ( $p_{FDR} < 0.01$ ). Finally, within 1 component of 3 nodes, patients with DPD showed lower FA values than controls between the left caudal anterior cingulate cortex and the left medial orbitofrontal cortex and higher FA values than controls between the latter and the right superior frontal gyrus ( $p_{FDR} < 0.01$ ).

### Partial correlation analyses

As 1 patient with DPD did not complete the CDS-30 questionnaire, data from 45 participants were analyzed with partial correlation analysis (controlling for age, sex and handedness). The link-based analysis yielded a significant negative correlation between DPD symptoms, as measured by the CDS-30, and FA values of 5 components (Appendix 1, Table S2). Four of these components match those identified in the group contrast for which patients with DPD showed lower FA values than controls when using a link-based controlling procedure (Table 3). In light of the high intercorrelations between questionnaires assessing anxiety, depression and dissociation, we tested whether this effect was driven by dissociation severity by performing additional partial correlation analyses with STAI-T scores and BDI scores. Using these as exclusive masks, we determined that mean FA between the left superior temporal gyrus and temporal pole (corrected  $\alpha$  level  $p_{FDR} < 0.001$ ) as well as mean FA between the right middle temporal gyrus and right supramarginal gyrus (corrected  $\alpha$  level  $p_{FDR} < 0.001$ ) correlate solely with dissociation severity. These results are shown and the respective scatterplots provided in Figure 3A–D.

**Table 3: Group comparison using link-based controlling procedure, controlled for age, sex and handedness\***

| Negative correlation between symptom scores and FA values |        |     | Significant components DPD $\neq$ HC†   | $p_{FDR}$ value |
|---|--------|-----|---|-----------------|
| BDI   | STAI-T | CDS |   |                 |
| —   | —      | √   | Left temporal pole -- Left superior temporal gyrus                                      | < 0.001         |
| —   | —      | √   | Right middle temporal gyrus -- Right supramarginal gyrus                                | 0.002           |
| —   | √      | √   | Brain stem -- Left Caudate  | < 0.001         |
| √   | √      | √   | Right medial OFC -- Right caudal ACC  | 0.001           |
| —   | √      | —   | Right inferior temporal gyrus -- Right lingual cortex                                   | < 0.001         |
| —   | —      | —   | Right superior temporal gyrus + + Right banks of superior temporal sulcus               | < 0.01          |
| —   | —      | —   | Left insula -- Left pars triangularis -- Left lateral OFC                               | < 0.01          |
| —   | —      | —   | Left caudal ACC -- Left medial OFC + + Right superior frontal gyrus                     | < 0.01          |
| —   | —      | —   | Left isthmus of the cingulate cortex + + Right cuneus + + Left superior parietal cortex | < 0.01          |

ACC = anterior cingulate cortex; BDI = Beck Depression Inventory; CDS = Cambridge Depersonalization Scale; DPD = depersonalization/derealization disorder; FA = fractional anisotropy; FDR = false discovery rate; HC = healthy controls; STAI-T = State-Trait Anxiety Scale, trait version; OFC = orbitofrontal cortex.

\*All components for which patients with DPD and controls displayed significantly different FA values are listed along with the respective  $p$  value. Ticks mark components for which a significant correlation was found with dissociative symptoms scores (CDS-30), trait anxiety (STAI-T), or depression (BDI).

†Minus signs between brain regions (--) represent connections for which patients with DPD displayed lower FA values than controls; plus signs between regions (+ +) represent connections for which patients displayed higher FA values than controls.

### Additional post hoc analyses

We performed additional post hoc analyses to control for potential effects of psychotropic medications, which were taken by 9 patients. We repeated the group comparison with medication as a covariate (in addition to age, sex and handedness) using NBS ( $p_n = 0.005$ ) and a link-based controlling procedure. Our main findings remained the same, even when medication effects were partialled out (Appendix 1, Table S3 and Table S4). Furthermore, we ran post hoc correlations within the patient group for age at symptom onset as well as duration of symptoms to verify whether components found in the group comparison could be further explained by these variables. In addition, we contrasted a subsample of patients without comorbid disorders ( $n = 11$ ) with healthy controls

( $n = 23$ ) to test whether FA values between certain regions might be associated exclusively with the DPD diagnosis. None of our post hoc analyses yielded any overlap between the subnetwork and graph components identified in the group comparison.

### Discussion

To our knowledge, this is the first study exploring aberrations in structural connectivity in patients with DPD. Two statistical correction methods for multiple comparisons were used to identify potential group differences in an explorative approach. Using link-based analysis, significant group differences were found for 9 links. Connections between the left superior temporal gyrus and the left temporal pole as well as

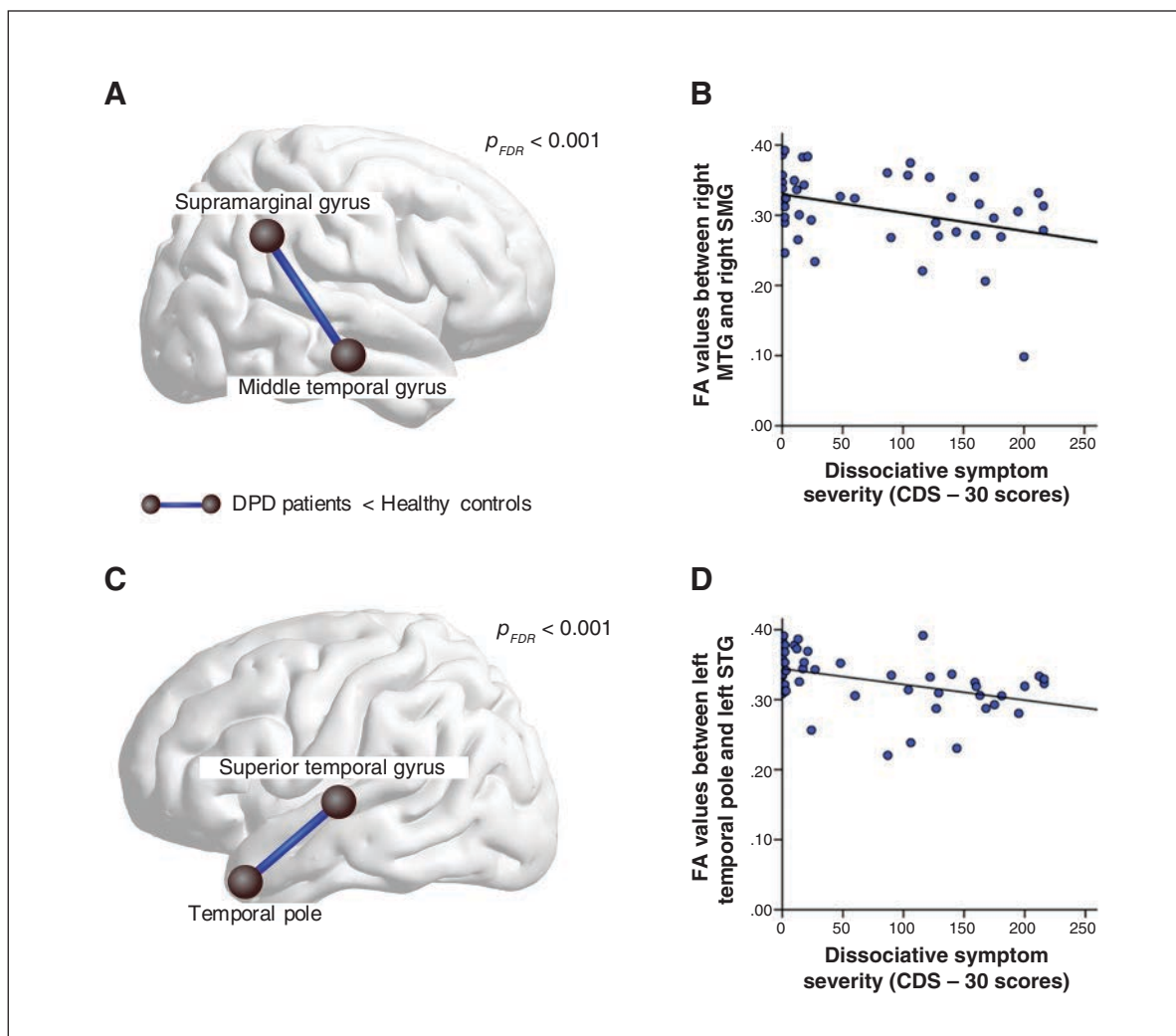


**Fig. 3:** Visualization of the 2 most outstanding results of the group comparison when using a link-based controlling procedure. First, **(A)** patients with depersonalization/derealization disorder (DPD) showed significantly lower fractional anisotropy (FA) between the right middle temporal gyrus and the right supramarginal gyrus. **(B)** The FA values within this connection were negatively correlated with dissociative symptom scores across groups, as measured by the CDS-30. Second, **(C)** relative to controls, patients with DPD showed significantly lower FA values between the left temporal pole and the left superior temporal gyrus. **(D)** Dissociative symptom severity correlated negatively with FA values of this connection. CDS = Cambridge Depersonalization Scale; FDR = false discovery rate; MTG = middle temporal gyrus; SMG = supramarginal gyrus; STG = superior temporal gyrus.

between the right middle temporal gyrus and the right supramarginal gyrus are characterized by lower mean FA values in the DPD group, which correlate with dissociative symptom severity, but not with anxiety or depressive symptom severity. The remaining 7 links do not correlate with dissociation severity exclusively; some showed significant correlations with both dissociation severity and anxiety or depression scores, whereas others did not correlate with either. Using NBS, a trend-level finding points toward connectivity alterations in a circuit comprising frontolimbic as well as subcortical striatal-brainstem connections, which partially overlap with connections identified when using link-based statistics.

The results from the link-based controlling procedure are discussed first. Altered structural connectivity (lower FA) in patients with DPD relative to controls was found between the right middle temporal gyrus (MTG) and the right supramarginal gyrus (SMG). In previous studies, lower metabolic rate<sup>13</sup> and reduced cortical thickness were reported for the right MTG in patients with DPD relative to controls,<sup>12</sup> whereas the SMG has previously been associated with dissociation in the context of PTSD.<sup>61</sup> As part of the somatosensory association cortex in the parietal lobe, the SMG receives input from visual, auditory, somatosensory and limbic structures; the right hemispheric SMG has been associated with cross-modal spatial attention<sup>62</sup> and sense of agency.<sup>63</sup> The function of the MTG is still unclear. It has been associated with conceptual processing<sup>64,65</sup> and transmodal integration,<sup>66,67</sup> but also with social anxiety<sup>68</sup> and hallucinations in schizophrenia.<sup>69,70</sup> Considering patients with DPD frequently report symptoms related to impaired integration of different sensory modalities as well as somatosensory distortions, alterations in fibre pathways between the right MTG and right SMG may represent the neuronal underpinnings of failed sensory integration necessary for, for example, an intact body perception in space.

Our second prominent finding using link-based analysis indicates lower structural connectivity between the left temporal pole and the left superior temporal gyrus, which is also in relative concordance with previous findings. Hollander and colleagues<sup>10</sup> found increased theta slowing in left temporal areas in a case study of DPD, and Sierra and colleagues<sup>12</sup> reported a significant correlation between dissociative symptom scores in DPD with the left inferior temporal gyrus. Furthermore, depersonalization symptoms have been associated with temporal lobe epilepsy, more often with left-sided foci,<sup>6</sup> and with electroencephalography abnormalities above the temporal lobe within the context of panic disorder.<sup>11,71</sup> The results of the present study extend these findings by highlighting the role of anatomic connections between the left superior temporal gyrus and the left temporal pole. In healthy individuals, the left superior temporal gyrus has been confirmed to play a role in auditory processing and language comprehension.<sup>72</sup> The temporal pole has been suggested to be an amodal “semantic hub,” which is crucial for forming associations across distinct attributes.<sup>73</sup> It is possible that reduced connectivity between these 2 temporal structures underlies dysfunctional association of multimodal information ob-

served in patients with DPD. In conjunction, these explorative findings suggest that the temporal lobe model of DPD<sup>9</sup> is worth pursuing further.

Moreover, potentially lower structural connectivity between the right medial OFC and right caudal ACC found in patients was associated with dissociative, anxiety and depressive symptoms and thus might be of particular interest from a transdiagnostic perspective. Finally, we further found 5 components pointing toward altered structural connectivity in right temporal regions, bilateral frontal and limbic areas as well as in left parietal and occipital cortices in patients with DPD relative to controls. However, no correlations between interregional FA values and symptom severity emerged, so these links seem to be less central to any neurobiological model of DPD.

Patients also showed relatively lower FA than controls between the brainstem and the left caudate, which was associated with dissociative scores as well as anxiety scores. This finding seems particularly important as it was also identified using NBS: this subnetwork was characterized by higher FA between frontal regions and projections to the amygdala and lower FA values between the amygdala, brainstem and left caudate (Fig. 2). According to the model of frontolimbic dysbalance,<sup>14,15</sup> prefrontal cortices are assumed to overregulate limbic structures,<sup>14</sup> resulting in the emotional numbing observed in patients with DPD. Albeit only approaching statistical significance in the current sample, this finding supports the frontolimbic dysbalance theory, as we found a trend toward higher structural connectivity (i.e., higher FA) within the left superior frontal gyrus and the right orbitofrontal cortex (OFC) and higher connectivity strength between the OFC and the amygdala in the DPD group. The OFC and the basolateral nucleus of the amygdala are important nodes in the limbic corticostriatal loop and share many reciprocal connections that have been associated with regulating emotional responses.<sup>74</sup> Frontolimbic inhibition has been reported in functional connectivity studies in PTSD and its dissociative subtype<sup>15</sup> and was confirmed in task-based fMRI in DPD, yet so far only in small samples.<sup>17–19</sup> Interestingly, the identified subnetwork also comprised connections in which patients with DPD showed lower mean FA values (between the brainstem to the right amygdala and the left caudate, respectively). Functional synchronization between the amygdala, caudate and medial prefrontal cortex has been suggested to subservise active coping with threat.<sup>75</sup> Accordingly, altered functional connectivity due to altered structural connectivity can be hypothesized to underlie passive responses to threat, such as dissociation. The primary control centre for internal and external stressors in the brainstem is the periaqueductal gray. Its connectivity with the central nucleus of the amygdala is suggested to play a role in freezing, a passive threat response, which is suggested to be the homologue of dissociation in animals.<sup>76</sup> Convergenly, dissociation in PTSD has been linked to reduced functional connectivity between the periaqueductal gray and the amygdala,<sup>77</sup> while activation of the caudate and the amygdala has been associated with specific dissociative identity states.<sup>78</sup> These distinct brain aberrations may be mediated by altered white matter on a network level. Thus, our findings suggest that

structural alterations in frontolimbic–striatal circuits may contribute to abnormal fear responses (e.g., emotional numbing) observed in DPD. However, as dissociative symptom severity was not significantly correlated with this network's FA values, future studies should carefully explore its role.

As for the question whether the reported group differences are best considered a diathesis for or a result of the disorder, we can only speculate. We could not confirm a relationship between FA values and duration of illness, but cannot rule out that this is due to the bimodal distribution of the duration of illness in our sample. Finally, as our results do not overlap with findings in the same cohort on grey matter alterations,<sup>20</sup> we assume that altered structural connectivity is best understood as a primary pathophysiology and not merely a secondary effect of local grey matter volume loss in patients with DPD.

### Limitations

The following limitations need to be considered. First, the present study is of a purely exploratory nature; that is, it represents a data-driven approach aimed at theory-building. Second, to ensure ecological validity, we did not exclude patients with comorbid disorders or patients taking psychotropic medication. It remains unclear whether the observed alterations in white matter fibre connections represent a risk factor or a consequence of the disorder due to the cross-sectional nature of this study. Finally, general methodological issues concerning the graph theoretical analysis of diffusion MRI tractography data apply. We used CSD tractography, which is capable of resolving crossing fibre tracts,<sup>79</sup> to reconstruct structural brain networks, decreasing the number of false-negative findings.<sup>80</sup> However, other difficulties of the tracking algorithm, such as modelling different fibre geometries and a potential increase of false-positive streamlines, need to be considered. By having included only links for which streamlines have been generated for all participants, we again reduced the influence of false-positive streamlines on the results. However, this procedure may have excluded relevant connections for the group contrast. In addition, it should be kept in mind that by using the diffusion parameter FA as an edge weight for the connectivity matrices, no strong inferences of the state of the anatomic connection between any 2 regions of interest can be made. Fractional anisotropy is modulated by a range of microstructural factors and the indication of lower or higher FA values in regard to the degree of structural connectivity remains unclear.<sup>81</sup> Finally, the resolution of the data and FreeSurfer parcellation limits the interpretation; e.g., we cannot ascertain which specific subnuclei of the amygdala and structures of the brainstem are involved in the detected network.

### Conclusion

This exploratory study is, to our knowledge, the first to report altered structural connectivity (i.e., FA values) in individuals with DPD compared with healthy controls. Our results support the model of frontolimbic dysbalance suggested to underlie emotional numbing in individuals

with DPD, while at the same time emphasizing the role of the temporal lobes, as suggested by an early conceptualization of the disorder.<sup>9</sup> We conclude that dysfunctional interaction on a network level as well as abnormal fibre tract connectivity on a link-based level, may contribute to the heterogenic symptomatology observed in individuals with DPD, which might also inform a transdiagnostic perspective.

Clinical implications could potentially be drawn from our findings in the long-term. One emphasis may lie in strengthening multimodal integration and embodiment in DPD. For severe and chronic courses, an interesting consideration on doing so refers to the implementation of repetitive transcranial magnetic stimulation above temporoparietal regions. In a first clinical trial, Mantovani and colleagues<sup>82</sup> reported significant symptom reduction in 6 of 12 participants after 3 weeks of low-frequency repetitive transcranial magnetic stimulation on the right temporoparietal junction, with the strongest improvement observed in anomalous body experiences (71% improvement in responders<sup>83</sup>). However, having used an exploratory approach, our results as well as their implications ought to be verified in a confirmatory study.

**Acknowledgements:** This work was funded by the grant II/84051 from the Volkswagen Foundation to H. Walter, the German Research Foundation (DFG) grant DA 1222/4-1 to J.K. Daniels, the EU Rosalind-Franklin Fellowship Program to J.K. Daniels, and the German National Merit Foundation grant to A. Sierk. The research of A. Leemans is supported by VIDI Grant 639.072.411 from the Netherlands Organisation for Scientific Research (NWO). The authors thank Lea Waller for technical support regarding the usage of GraphVar.

**Affiliations:** From the Charité – Universitätsmedizin Berlin, corporate member of Freie Universität Berlin, Humboldt-Universität zu Berlin, and Berlin Institute of Health, Berlin, Germany (Sierk, Manthey, Lamke, Kruschwitz, Walter); the Institute of Cognitive Neuroscience, University College London, London, UK (Sierk); the Department of Clinical Psychology, University of Groningen, Groningen, The Netherlands (Daniels); the Department of Neurology, University of Groningen, University Medical Center Groningen, The Netherlands (Kok); the PROVIDI Lab, University Medical Center Utrecht, Utrecht, the Netherlands (Leemans); and the Max Planck Institute for Human Cognitive and Brain Sciences, Leipzig, Germany (Gaebler).

**Competing interests:** J.-P. declares personal fees from BIOTRONIK SE & Co. KG, outside the submitted work. No other competing interests declared.

**Contributors:** J. Daniels, M. Gaebler, J.-P. Lamke and H. Walter designed the study. J. Daniels, M. Gaebler and J.-P. Lamke acquired the data, which A. Sierk, J. Daniels, A. Manthey, J. Kok, A. Leemans and J. Kruschwitz analyzed. A. Sierk wrote the article, which all authors reviewed. All authors approved the final version to be published and can certify that no other individuals not listed as authors have made substantial contributions to the paper.

### References

1. American Psychiatric Association. *Diagnostic and statistical manual of mental disorders (DSM-5®)*. Philadelphia (PA): APA; 2013.
2. Hunter EC, Sierra M, David AS. The epidemiology of depersonalisation and derealisation. A systematic review. *Soc Psychiatry Psychiatr Epidemiol* 2004;39:9-18.
3. Michal M, Beutel ME, Grobe TG. Wie oft wird die Depersonalisations-Derealisationsstörung (ICD-10: F48.1) in der ambulanten Versorgung diagnostiziert? *Zeitschrift für Psychosomatische Medizin und Psychotherapie*, 2010;56:74-83.

4. Baker D, Hunter E, Lawrence E, et al. Depersonalisation disorder: clinical features of 204 cases. *Br J Psychiatry* 2003;182:428-33.
5. Michal M, Adler J, Wiltink J, et al. A case series of 223 patients with depersonalization-derealization syndrome. *BMC Psychiatry* 2016; 16:203.
6. Devinsky O, Putnam F, Grafman J, et al. Dissociative states and epilepsy. *Neurology* 1989;39:835-40.
7. Ross CA, Keyes B. Dissociation and Schizophrenia. *J Trauma Dissociation* 2004;5:69-83.
8. Daniels JK, Coupland NJ, Hegadoren KM, et al. Neural and behavioral correlates of peritraumatic dissociation in an acutely traumatized sample. *J Clin Psychiatry* 2012;73:420-6.
9. Penfield, W. and T. Rasmussen, The cerebral cortex of man; a clinical study of localization of function. 1950.
10. Hollander E, Carrasco JL, Mullen LS, et al. Left hemispheric activation in depersonalization disorder: a case report. *Biol Psychiatry* 1992; 31:1157-62.
11. Locatelli M, Bellodi L, Perna G, et al. EEG power modifications in panic disorder during a temporolimbic activation task: relationships with temporal lobe clinical symptomatology. *J Neuropsychiatry Clin Neurosci* 1993;5:409-14.
12. Sierra M, Nestler S, Jay EL, et al. A structural MRI study of cortical thickness in depersonalisation disorder. *Psychiatry Res* 2014;224:1-7.
13. Simeon D, Guralnik O, Hazlett EA, et al. Feeling unreal: a PET study of depersonalization disorder. *Am J Psychiatry* 2000;157:1782-8.
14. Sierra M, Berrios GE. Depersonalization: neurobiological perspectives. *Biol Psychiatry* 1998;44:898-908.
15. Lanius RA, Vermetten E, Loewenstein RJ, et al. Emotion modulation in PTSD: Clinical and neurobiological evidence for a dissociative subtype. *Am J Psychiatry* 2010;167:640-7.
16. Lemche E, Anilkumar A, Giampietro VP, et al. Cerebral and autonomic responses to emotional facial expressions in depersonalisation disorder. *Br J Psychiatry* 2008;193:222-8.
17. Phillips ML, Medford N, Senior C, et al. Depersonalization disorder: thinking without feeling. *Psychiatry Res* 2001;108:145-60.
18. Medford N, Brierley B, Brammer M, et al. Emotional memory in depersonalization disorder: a functional MRI study. *Psychiatry Res* 2006;148:93-102.
19. Medford N, Sierra M, Stringaris A, et al. Emotional experience and awareness of self: functional MRI studies of depersonalization disorder. *Front Psychol* 2016;7:432.
20. Daniels JK, Gaebler M, Lamke JP, et al. Grey matter alterations in patients with depersonalization disorder: a voxel-based morphometry study. *J Psychiatry Neurosci* 2015;40:19-27.
21. Nicholson AA, Densmore M, Frewen PA, et al. The dissociative subtype of posttraumatic stress disorder: unique resting-state functional connectivity of basolateral and centromedial amygdala complexes. *Neuropsychopharmacology* 2015;40:2317-26.
22. Edelman GM, Tononi G. *A universe of consciousness: How matter becomes imagination*. 2000: Basic books.
23. Sedeño L, Couto B, Melloni M, et al. How do you feel when you can't feel your body? Interoception, functional connectivity and emotional processing in depersonalization-derealization disorder. *PLoS One* 2014;9:e98769.
24. Jones DK, Leemans A. Diffusion tensor imaging. In: Modo M, Bulte JWM, editors, *Magnetic resonance neuroimaging: methods and protocols*. Totowa (NJ): Humana Press; 2011 p. 127-144.
25. Tournier J-D, Mori S, Leemans A. Diffusion tensor imaging and beyond. *Magn Reson Med* 2011;65:1532-56.
26. Hagmann P, Kurant M, Gigandet X, et al. Mapping human whole-brain structural networks with diffusion MRI. *PLoS One* 2007;2:e597.
27. Bullmore E, Sporns O. Complex brain networks: graph theoretical analysis of structural and functional systems. *Nat Rev Neurosci* 2009;10:186-98.
28. Fornito A, Zalesky A, Breakspear M. Graph analysis of the human connectome: promise, progress, and pitfalls. *Neuroimage* 2013;80: 426-44.
29. Griffa A, Baumann PS, Thiran JP, et al. Structural connectomics in brain diseases. *Neuroimage* 2013;80:515-26.
30. Zalesky A, Fornito A, Bullmore ET. Network-based statistic: identifying differences in brain networks. *Neuroimage* 2010;53:1197-207.
31. Szucs D, Ioannidis JPA. When null hypothesis significance testing is unsuitable for research: a reassessment. *Front Hum Neurosci* 2017;11:390.
32. Gast U, Zündorf F, Hofmann A. *Strukturiertes klinisches Interview für DSM-IV-dissoziative Störungen (SKID-D): Manual*. Hogrefe, Verlag für Psychologie; 2000.
33. Wittchen H, Zaudig M, Schramm E, et al. *Das Strukturierte Klinische Interview nach DSM-IV*. Beltz: Weinheim; 1996.
34. Mombour W, Zaudig M, Berger P, et al. International Personality Disorder Examination (IPDE). Hogrefe Testzentrale, Göttingen; 1996.
35. Michal M, Sann U, Niebecker M, et al., Die Erfassung des Depersonalisations-Derealisations-Syndroms mit der Deutschen Version der Cambridge Depersonalisation Scale (CDS). *PPmP-Psychotherapie. Psychosomatik Medizinische Psychologie*; 2004. p. 367-374.
36. Spitzer C, Mestel R, Klingelhöfer J, et al. Screening and measurement of change of dissociative psychopathology: psychometric properties of the short version of the Fragebogen zu Dissoziativen Symptomen (FDS-20). *Psychother Psychosom Med Psychol* 2004;54:165-72.
37. Hautzinger M, Keller F, Kühner C. Beck-Depressions-Inventar: Revision. 2006: Harcourt Test Services.
38. Laux L, Spielberger CD. Das state-trait-angstinventar: STAI. 2001: Beltz Test Göttingen.
39. Stangier U, Heidenreich T. Die Liebowitz Soziale Angst-Skala (LSAS). Skalen für Psychiatrie, 2003.
40. Bach M, Bach D, de Zwaan M, et al. Validierung der deutschen Version der 20-Item Toronto-Alexithymie-Skala bei Normalpersonen und psychiatrischen Patienten. *Psychother Psychosom Med Psychol* 1996;46:23-8.
41. Abler B, Kessler H. Emotion Regulation Questionnaire—Eine deutschsprachige Fassung des ERQ von Gross und John. *Diagnostica* 2009;55:144-52.
42. Ströhle G, Nachtigall C, Michalak J, et al. Die Erfassung von Achtsamkeit als mehrdimensionales Konstrukt. *Z Klin Psychol Psychother* 2010.
43. Hoyer J. Der Fragebogen zur Dysfunktionalen und Funktionalen Selbstaufmerksamkeit (DFS): Theoretisches Konzept und Befunde zur Reliabilität und Validität. *Diagnostica* 2000;46:140-8.
44. Gräfe K. Sheehan Disability Scale (SDS). *Angstdiagnostik*. Springer, Berlin, 2003: p. 158-160.
45. Wingenfeld K, Spitzer C, Mensebach C, et al., Die deutsche Version des Childhood Trauma Questionnaire (CTQ): Erste Befunde zu den psychometrischen Kennwerten. *PPmP-Psychotherapie-Psychosomatik- Medizinische Psychologie*, 2010;60: 442-50.
46. Stanczak DE, Lynch MD, McNeil CK, et al. The expanded trail making test: rationale, development, and psychometric properties. *Arch Clin Neuropsychol* 1998;13:473-87.
47. Fischl B, Dale AM. Measuring the thickness of the human cerebral cortex from magnetic resonance images. *Proc Natl Acad Sci U S A* 2000;97:11050-5.
48. Leemans A, Jeurissen B, Sijbers J, et al. ExploreDTI: a graphical toolbox for processing, analyzing, and visualizing diffusion MR data. *Proceedings of the 17th Annual Meeting of Intl Soc Magn Reson Med*. 2009.
49. Tax CM, Otte WM, Viergever MA, et al. REKINDLE: robust extraction of kurtosis INDices with linear estimation. *Magn Reson Med* 2015;73:794-808.
50. Leemans A, Jones DK. The B-matrix must be rotated when correcting for subject motion in DTI data. *Magn Reson Med* 2009;61:1336-49.
51. Irfanoglu MO, Walker L, Sarlls J, et al. Effects of image distortions originating from susceptibility variations and concomitant fields on diffusion MRI tractography results. *Neuroimage* 2012;61:275-88.
52. Jeurissen B, Leemans A, Jones DK, et al. Probabilistic fiber tracking using the residual bootstrap with constrained spherical deconvolution. *Hum Brain Mapp* 2011;32:461-79.
53. Tax CM, Jeurissen B, Vos SB, et al. Recursive calibration of the fiber response function for spherical deconvolution of diffusion MRI data. *Neuroimage* 2014;86:67-80.
54. Jeurissen B, Descoteaux M, Mori S, et al. Diffusion MRI fiber tractography of the brain. *NMR Biomed* 2017; doi: 10.1002/nbm.3785 [Epub ahead of print].
55. Maier-Hein KH, Neher PF, Houde JC, et al. The challenge of mapping the human connectome based on diffusion tractography. *Nat Commun* 2017;8:1349.
56. Gong G, Rosa-Neto P, Carbonell F, et al. Age- and gender-related differences in the cortical anatomical network. *J Neurosci* 2009;29:15684-93.
57. Hasan KM, Alexander AL, Narayana PA. Does fractional anisotropy have better noise immunity characteristics than relative anisotropy in diffusion tensor MRI? An analytical approach. *Magn Reson Med* 2004;51:413-7.

58. Kruschwitz JD, List D, Waller L, et al. GraphVar: a user-friendly toolbox for comprehensive graph analyses of functional brain connectivity. *J Neurosci Methods* 2015;245:107-15.
59. Genovese C, Wasserman L. Operating characteristics and extensions of the false discovery rate procedure. *J R Stat Soc Series B Stat Methodol* 2002;64:499-517.
60. Benjamini Y, Yekutieli D. The control of the false discovery rate in multiple testing under dependency. *Ann Stat* 2001;29:1165-88.
61. Harricharan S, Nicholson AA, Densmore M, et al. Sensory overload and imbalance: Resting-state vestibular connectivity in PTSD and its dissociative subtype. *Neuropsychologia* 2017;106(Supplement C):169-78.
62. Macaluso E, Frith CD, Driver J. Modulation of human visual cortex by crossmodal spatial attention. *Science* 2000;289:1206-8.
63. Farrer C, Franck N, Georgieff N, et al. Modulating the experience of agency: a positron emission tomography study. *Neuroimage* 2003;18:324-33.
64. Friederici AD, Ruschemeyer SA, Hahne A, et al. The role of left inferior frontal and superior temporal cortex in sentence comprehension: localizing syntactic and semantic processes. *Cereb Cortex* 2003;13:170-7.
65. Wei T, Liang X, He Y, et al. Predicting conceptual processing capacity from spontaneous neuronal activity of the left middle temporal gyrus. *J Neurosci* 2012;32:481-9.
66. Mesulam MM. From sensation to cognition. *Brain* 1998;121:1013-52.
67. Visser M, Jefferies E, Embleton KV, et al. Both the middle temporal gyrus and the ventral anterior temporal area are crucial for multimodal semantic processing: distortion-corrected fMRI evidence for a double gradient of information convergence in the temporal lobes. *J Cogn Neurosci* 2012;24:1766-78.
68. Yun JY, Kim JC, Ku J, et al. The left middle temporal gyrus in the middle of an impaired social-affective communication network in social anxiety disorder. *J Affect Disord* 2017;214:53-9.
69. McGuire PK, David A, Murray R, et al. Abnormal monitoring of inner speech: a physiological basis for auditory hallucinations. *Lancet* 1995;346:596-600.
70. Onitsuka T, Shenton ME, Salisbury DF, et al. Middle and inferior temporal gyrus gray matter volume abnormalities in chronic schizophrenia: an MRI study. *Am J Psychiatry* 2004;161:1603-11.
71. Hayashi K, Makino M, Hashizume M, et al. Electroencephalogram abnormalities in panic disorder patients: a study of symptom characteristics and pathology. *Biopsychosoc Med* 2010;4:9.
72. Buchsbaum BR, Hickok G, Humphries C. Role of left posterior superior temporal gyrus in phonological processing for speech perception and production. *Cogn Sci* 2001;25:663-78.
73. Patterson K, Nestor PJ, Rogers TT. Where do you know what you know? The representation of semantic knowledge in the human brain. *Nat Rev Neurosci* 2007;8:976-87.
74. Winstanley CA, Theobald DE, Cardinal RN, et al. Contrasting roles of basolateral amygdala and orbitofrontal cortex in impulsive choice. *J Neurosci* 2004;24:4718-22.
75. Collins KA, Mendelsohn A, Cain CK, et al. Taking action in the face of threat: neural synchronization predicts adaptive coping. *J Neurosci* 2014;34:14733-8.
76. Hageaars MA, Oitzl M, Roelofs K. Updating freeze: aligning animal and human research. *Neurosci Biobehav Rev* 2014;47:165-76.
77. Nicholson AA, Friston KJ, Zeidman P, et al. Dynamic causal modeling in PTSD and its dissociative subtype: Bottom-up versus top-down processing within fear and emotion regulation circuitry. *Hum Brain Mapp* 2017;38:5551-61.
78. Reinders AA, Willemsen AT, den Boer JA, et al. Opposite brain emotion-regulation patterns in identity states of dissociative identity disorder: a PET study and neurobiological model. *Psychiatry Res* 2014;223:236-43.
79. Jeurissen B, Leemans A, Tournier JD, et al. Investigating the prevalence of complex fiber configurations in white matter tissue with diffusion magnetic resonance imaging. *Hum Brain Mapp* 2013;34:2747-66.
80. Tournier JD, Calamante F, Connelly A. Robust determination of the fibre orientation distribution in diffusion MRI: non-negativity constrained super-resolved spherical deconvolution. *Neuroimage* 2007;35:1459-72.
81. Jones DK, Knosche TR, Turner R. White matter integrity, fiber count, and other fallacies: the do's and don'ts of diffusion MRI. *Neuroimage* 2013;73:239-54.
82. Mantovani A, Simeon D, Urban N, et al. Temporoparietal junction stimulation in the treatment of depersonalization disorder. *Psychiatry Res* 2011;186:138-40.
83. Christopheit M, Simeon D, Urban N, et al. Effects of repetitive transcranial magnetic stimulation (rTMS) on specific symptom clusters in depersonalization disorder (DPD). *Brain Stimul* 2014;7:141-3.